Retinoic acid worsens Atg10-dependent autophagy impairment in TBK1-mutant hiPSC-derived motoneurons through SQSTM1/p62 accumulation.

Alberto Catanese[1,2], Florian olde Heuvel[3], Medhanie Mulaw[4], Maria Demestre[1], Julia Higelin[1,2], Gotthold Barbi[5], Axel Freischmidt[3], Jochen H Weishaupt[3], Albert C Ludolph[3], Francesco Roselli[1,3,6], Tobias M Boeckers[1,6]

Affiliations:
1. Institute of Anatomy and Cell Biology, Ulm University, Ulm (DE)
2. International Graduate School, Ulm University, Ulm (DE)
3. Dept. of Neurology, Ulm University, Ulm (DE)
4. Institute of Experimental Tumor Research, Ulm University, Ulm (DE)
5. Institute for Human Genetics, Ulm University Ulm, Germany (DE)
6. Co-senior authors

Corresponding author: Tobias M. Boeckers

Institute of Anatomy and Cell Biology,

Albert-Einstein Allee 11-89081 Ulm

Tel: 0731-500-23221/0

Fax: 0731-500-23217

Email: tobias.boeckers@uni-ulm.de

This file contains 7 Supplementary Figures

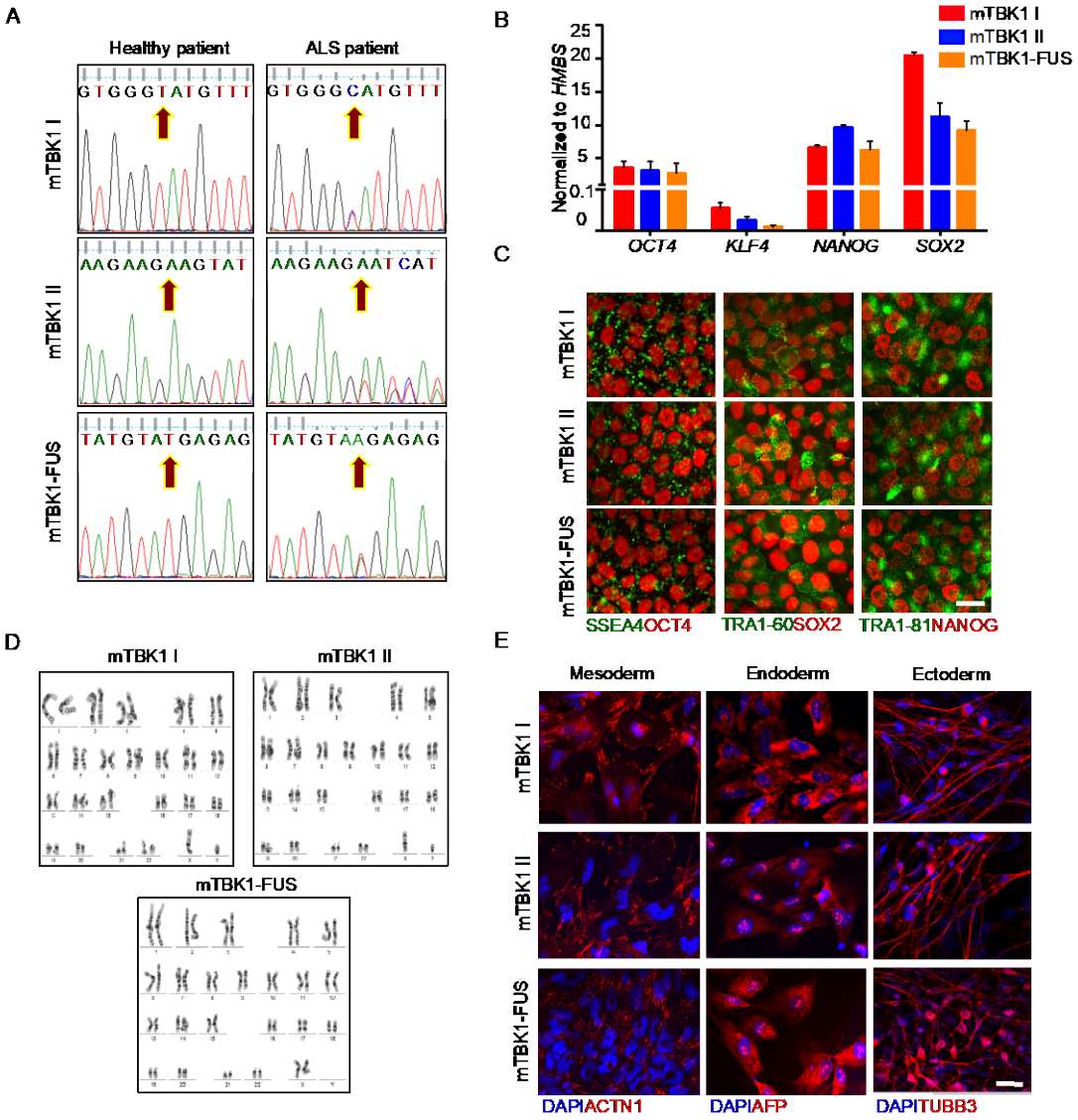

Figure S1. Pluripotency characterization of mTBK1 hiPSCs. (**A**) mTBK1 hiPSCs maintained the genomic mutations after reprogramming. (**B**) qRT-PCR analysis of typical pluripotency markers mRNA expression in mTBK1 hiPSCs. (**C**) Representative immunolabeling of mTBK1 hiPSCs against typical pluripotency markers. (**D**) Analysis of mTBK1 hiPSCs' karyogramm does not reveal any aberration after reprogramming. (**E**) Representative immunolabeling of mTBK1 hiPSCs against typical markers of germ layers mesoderm, endoderm and ectoderm. Data information: the qRT-PCR and immunolabeling experiments were performed in N=3 independent cultures/differentiation. Scale bars: 10 µm in (**C**) and 25 µm in **(E)**. Data are presented as mean ± SEM.

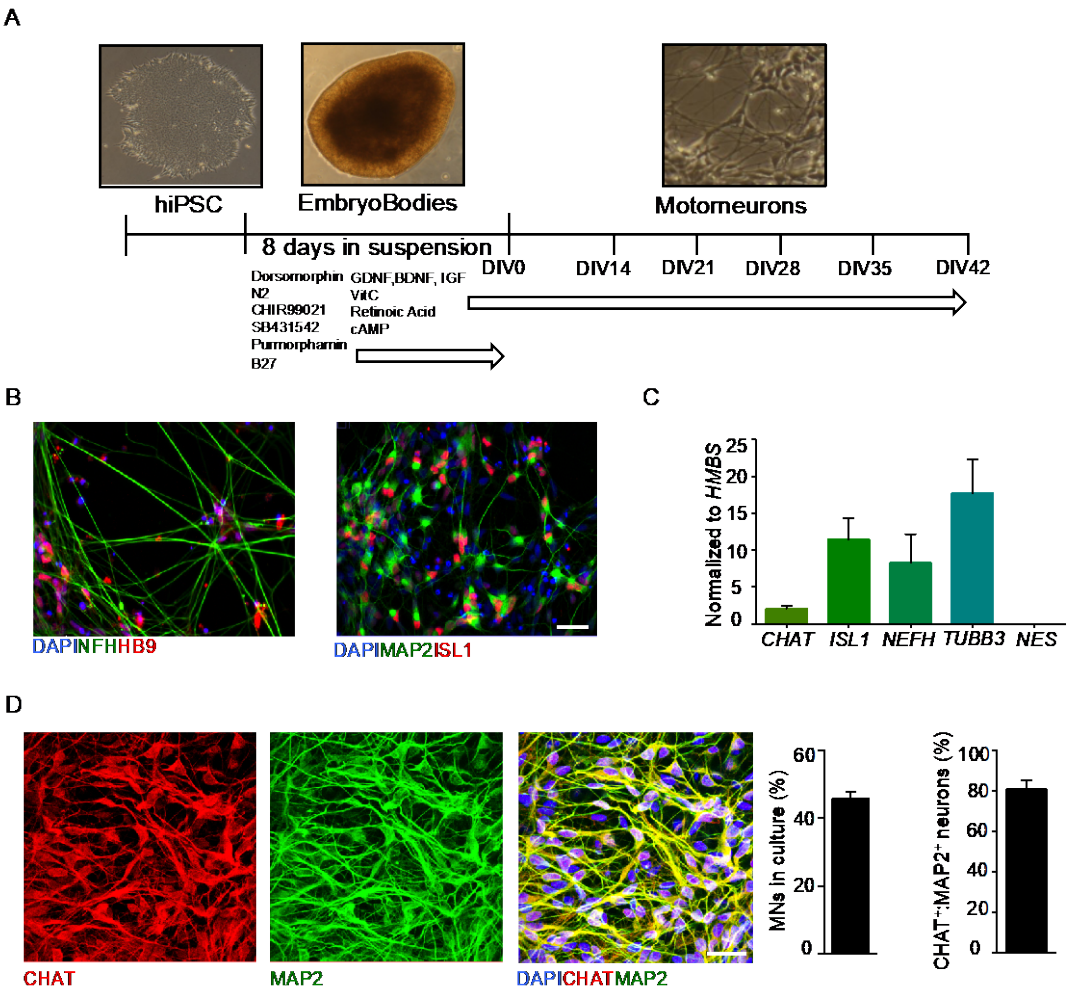

Figure S2. Characterization of differentiated MNs. (**A**) Schematic representation of MNs differentiation protocol. (**B**) Representative immunolabeling of differentiated MNs at DIV 14 against typical MNs markers. (**C**) qRT-PCR analysis of typical motor neuronal markers mRNA expression in differentiated MNs at DIV14. (**D**) Representative confocal image of MNs at DIV14 immunolabeled against CHAT and MAP2. With this protocol, 45% of efficiency was obtained in differentiating MNs. Moreover, among the neuronal cells obtained during the procedure, the majority was CHAT-positive (as shown by 80% of $MAP2^{+}$ cells being also positively stained against CHAT). Data information: experiments were performed in N=3 independent replicates. Scale bars: (**B** and **D**) 25 µm. Data are presented as mean ± SEM.

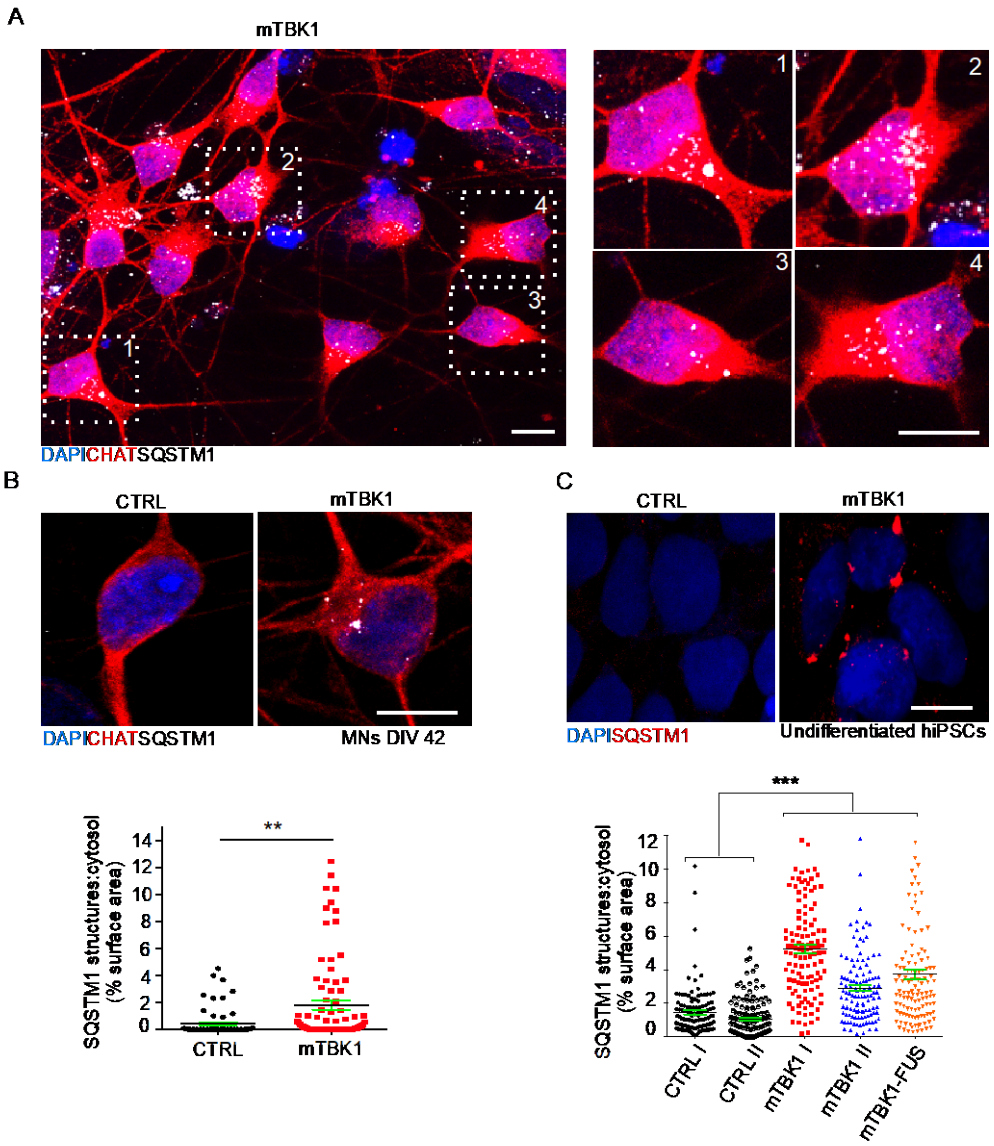

Figure S3. SQSTM1 accumulates in mTBK1 aged MNs and in undifferentiated hiPSCs. (**A**) Rapresentative confocal images of mTBK1 MNs at DIV14 displaying different degrees of SQSTM1 burden. (**B**) Representative confocal images of CTRL and mTBK1 MNs at DIV48 immunolabeled against CHAT and SQSTM1. Also in aged MNs, SQSTM1 accumulates within mTBK1 MNs somata (Mann Whitney test; **p<0.01). (**C**) Representative confocal images of CTRL and mTBK1 hiPSCs immunolabeled against SQSTM1. At the undifferentiated stage, mTBK1 hiPSCs show increased SQSTM1 accumulation in comparison to CTRL (one-way ANOVA followed by Sidak´s multiple comparisons test; ***p<0.001). Data information: immunocytochemistry was performed in N=3 independent replicates and a minimum of 60 $CHAT^{+}$ cells were analyzed in (**B**). In (**C**), a minimum of 100 hiPSCs was analyzed. To

improve readability, in (**C**) is displayed only the statistical comparison between the 2 genotypes. Scale bars: (**A** and **B**) 10 μm, (**C**) 5 μm. Data are presented as mean ± SEM.

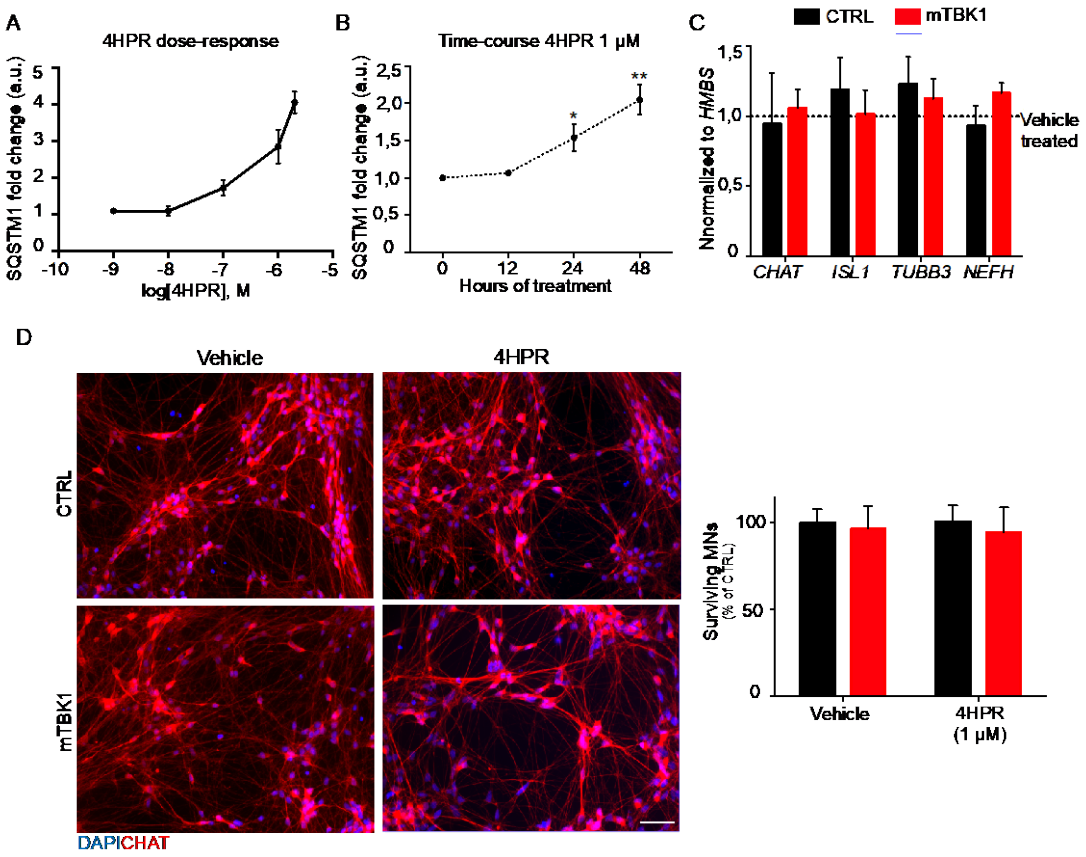

Figure S4. Characterization of 4HPR effect on MNs´ fitness**.** (**A**) Dose-response analysis of 4HPR treatment (24 h) on mTBK1 MNs at DIV14. The SQSTM1 signal intensity is increased starting at the concentration of 1 µM. (**B**) Time-course analysis of 4HPR (1 µM) treatment on mTBK1 MNs at DIV 14. Twenty-four h are sufficient to significantly increase the intensity of SQSTM1 signal (one-way ANOVA followed by Sidak´s multiple comparisons test; *p<0.05; **p<0.01)**.** (**C**) qRT-PCR analysis of typical motor neuronal markers expression levels in CTRL and mTBK1 MNs at DIV 14 treated with 4HPR (1 µM) for 24 h. 4HPR did not exert any significant effect on the markers investigated in both genotypes. (**D**) Representative immunolabeling of CTRL and mTBK1 MNs at DIV14, treated with 4HPR (1 µM) for 24 h and stained against CHAT. 4HPR does not affect the MNs viability in both genotypes. Data information: all the experiments were performed in N=3 independent replicates. For 4HPR dose-response and time-course experiments we analyzed a minimum of 90 MNs. To evaluate whether 4HPR might alter MN population, we manually analyzed a minimum of 1000 $DAPI^+$ nuclei and evaluated their positivity for CHAT staining in each genotype and treatment. Scale bar: 50 µm. Data are presented as mean ± SEM. a.u., arbitrary units.

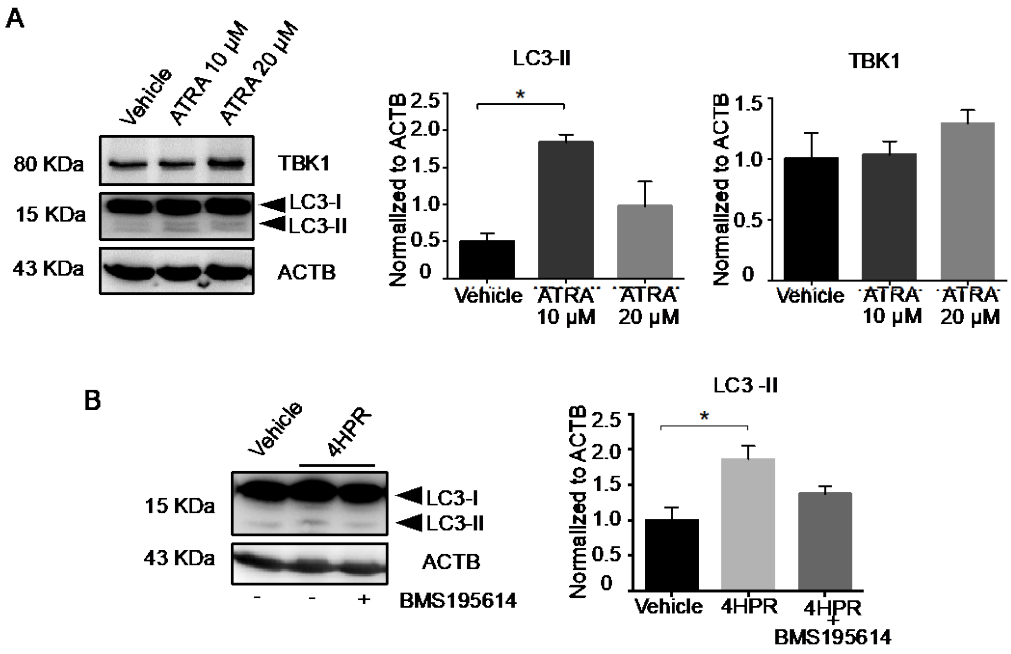

Figure S5. 4HPR induces autophagy by activating the RARA. (**A**) Immunoblot analysis of endogenous TBK1 and LC3-II protein levels in CTRL MNs at DIV14 treated with vehicle or ATRA (10 μM or 20 μM) for 24 h. As shown by 4HPR treatment, ATRA-mediated RARA activation induces autophagy by increasing the lipidation of LC3 (one-way ANOVA followed by Sidak´s multiple comparisons test; *p<0.05). No significant effect was detected on TBK1 protein levels. (**B**) Immunoblot analysis of endogenous LC3-II protein levels in CTRL MNs at DIV14 treated with vehicle, 4HPR (1 μM) or 4HPR (1 μM)+BMS195614 (50 μM) for 24 h. Co-treatment of MNs with 4HPR and RARA antagonist prevents autophagy induction detected by lipidation of LC3 (one-way ANOVA followed by Sidak´s multiple comparisons test; *p<0.05). Data information: the immunoblot experiments were performed in N=3 independent replicates. Data are presented as mean ± SEM.

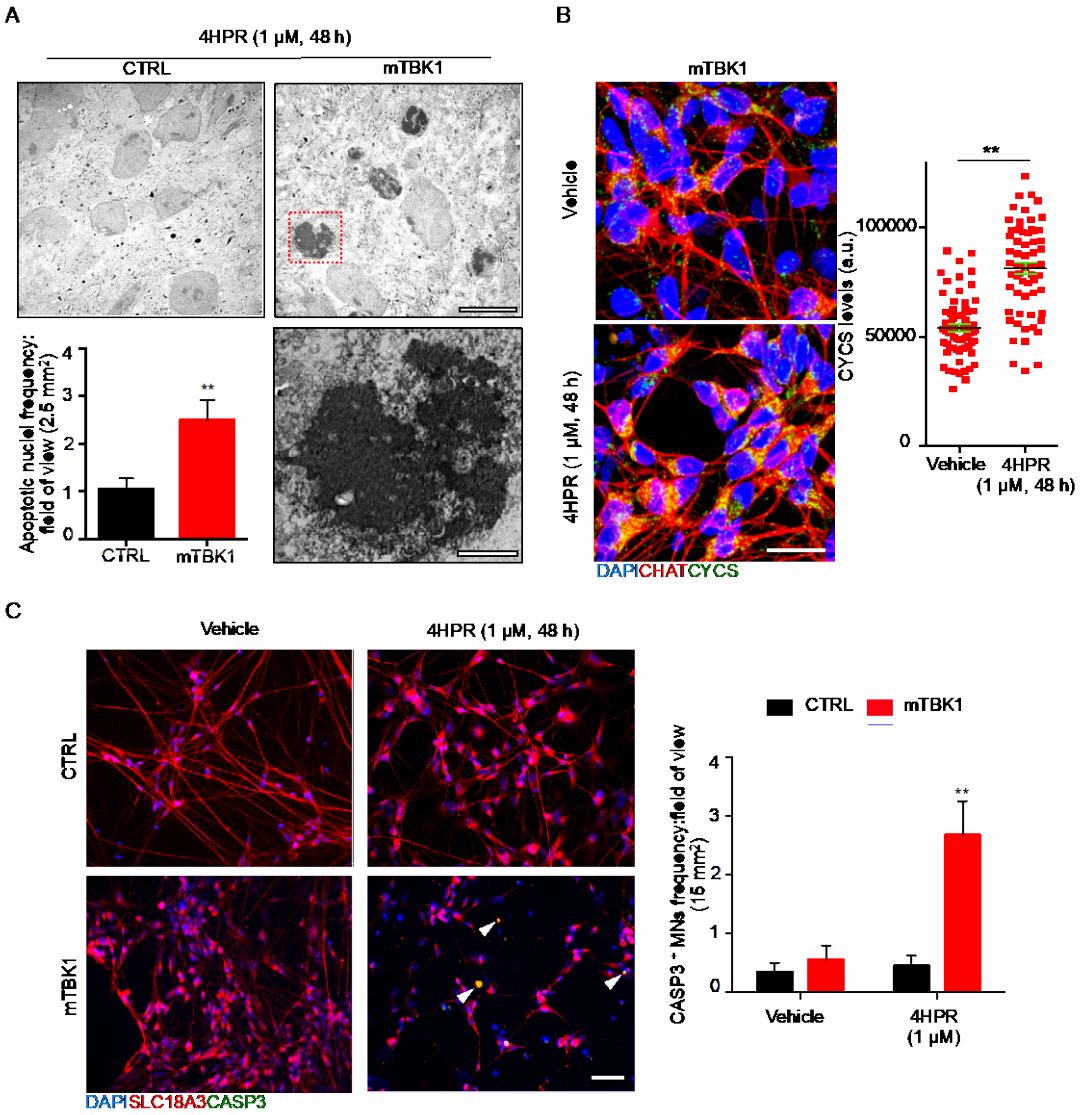

Figure S6. Longer 4HPR exposure increases cell death in mTBK1 MNs. (**A**) TEM analysis of CTRL and TBK1 MNs at DIV14 treated with 4HPR (1 µM) for 48 h. mTBK1 show a higher frequency of apoptotic nuclei (a representative apoptotic nucleus is highlighted in red and in a higher magnification beside) in comparison to CTRL (Mann Whitney test; **p<0.01). (**B**) Representative confocal images of mTBK1 MNs at DIV14 treated with 4HPR (1 µM) for 48 h and stained against CHAT and CYCS. Prolonged exposure to the retinoid induces a dramatic increase in CYCS levels. (**C**) Representative immunolabeling of CTRL and mTBK1 MNs at DIV14 treated with 4HPR (1 µM) for 48 h and stained against SLC18A3/VACHT and CASP3. 4HPR treatment increases the number of SLC18A3/VACHT-CASP3 double-positive cells in mTBK1 MNs (two-way ANOVA followed by Holm-Sidak´s multiple comparisons test 4HPR treated: **p<0.01). Data information: in (**B**) and (**C**) ICC was performed in N=3 independent

replicates; a minimum of 12 fields of view were acquired and all the cells inside it were evaluated. TEM analysis was performed on a minimum of 10 fields of view (from N=2 independent differentiations). Scale bars: (**A**) 10 μm in lower magnification and 2 μm in higher magnification; (**B** and **C**) 25 μm. Data are presented as mean ± SEM. a.u., arbitrary units.

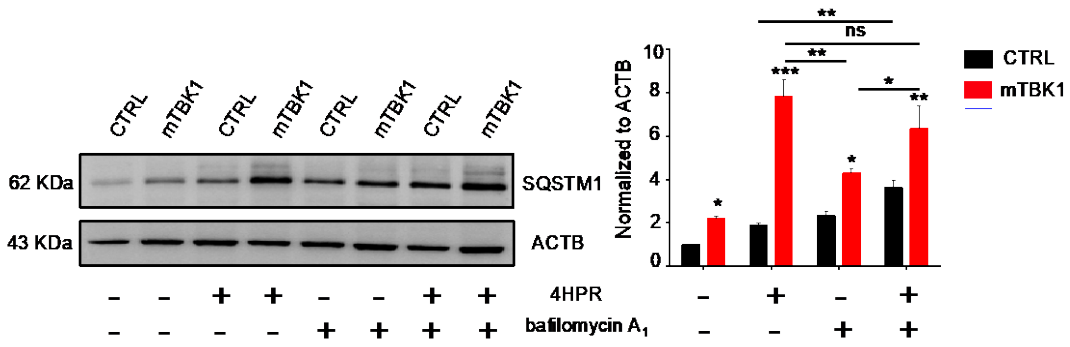

Figure S7. 4HPR induces SQSTM1 accumulation in mTBK1 upstream lysosomal fusion. Immunoblot analysis of endogenous SQSTM1 protein levels in CTRL and mTBK1 MNs at DIV14 treated with vehicle, 4HPR, bafilomycin A_1 or 4HPR+bafilomycin A_1 for 24 h. The accumulation of SQSTM1 triggered by 4HPR in mTBK1 MNs is higher then the accumulation driven by bafilomycin A_1, confirming that the impairment characterizing TBK1 mutants occurs at the early phases of autophagic flux (two-way ANOVA followed by Holm-Sidak´s multiple comparisons test 4HPR treated: *p<0.05; **p<0.01; ***p<0.001). Experiments were performed in N=3 independent replicates. Data are presented as mean ± SEM.